Supersensitivity to anandamide and enhanced endogenous cannabinoid signaling in mice lacking fatty acid amide hydrolase

Benjamin F. Cravatt*[†], Kristin Demarest*, Matthew P. Patricelli*, Michael H. Bracey*, Dan K. Giang*, Billy R. Martin[‡], and Aron H. Lichtman[‡]

*The Skaggs Institute for Chemical Biology and Departments of Cell Biology and Chemistry, The Scripps Research Institute, La Jolla, CA 92037; and [‡]Department of Pharmacology and Toxicology, Medical College of Virginia Campus, Virginia Commonwealth University, Richmond, VA 23298

The medicinal properties of marijuana have been recognized for centuries, but clinical and societal acceptance of this drug of abuse as a potential therapeutic agent remains fiercely debated. An attractive alternative to marijuana-based therapeutics would be to target the molecular pathways that mediate the effects of this drug. To date, these neural signaling pathways have been shown to comprise a cannabinoid receptor (CB_1) that binds the active constituent of marijuana, tetrahydrocannabinol (THC), and a postulated endogenous CB_1 ligand anandamide. Although anandamide binds and activates the CB_1 receptor *in vitro*, this compound induces only weak and transient cannabinoid behavioral effects *in vivo*, possibly a result of its rapid catabolism. Here we show that mice lacking the enzyme fatty acid amide hydrolase ($FAAH^{-/-}$) are severely impaired in their ability to degrade anandamide and when treated with this compound, exhibit an array of intense CB_1-dependent behavioral responses, including hypomotility, analgesia, catalepsy, and hypothermia. $FAAH^{-/-}$-mice possess 15-fold augmented endogenous brain levels of anandamide and display reduced pain sensation that is reversed by the CB_1 antagonist SR141716A. Collectively, these results indicate that FAAH is a key regulator of anandamide signaling *in vivo*, setting an endogenous cannabinoid tone that modulates pain perception. FAAH may therefore represent an attractive pharmaceutical target for the treatment of pain and neuropsychiatric disorders.

The endogenous cannabinoid system has been the focus of intense research over the past decade (1–3). Cannabinoid receptors that recognize the active component of marijuana, Δ^9-tetrahydrocannabinol (THC) (4), have been identified in both the brain (CB_1 receptor) and immune system (CB_2 receptor) (5). Additionally, a natural brain lipid, *N*-arachidonoyl ethanolamine, or anandamide, has been characterized as a possible endogenous ligand for the CB_1 receptor (6). Consistent with its postulated role as an endocannabinoid, anandamide (*i*) binds and activates the CB_1 receptor *in vitro* (6, 7), (*ii*) is produced in the brain in response to peripheral pain stimuli (8), and (*iii*) induces some cannabinoid behavioral effects *in vivo*, including hypothermia, analgesia, and motor defects (9–11).

Although a number of biochemical and cell biological studies have provided evidence that anandamide acts as an endogenous CB_1 ligand (6, 7, 12, 13), the behavioral effects induced by this compound are very weak and transient, especially when compared with those elicited by exocannabinoids like THC (11). Additionally, efforts to block the behavioral effects of anandamide with the CB_1 antagonist SR141716A have met with mixed success (14, 15). Most recently, anandamide was found to produce significant behavioral effects in CB_1 receptor-knockout ($CB_1^{-/-}$) mice (16), suggesting that an alternative site(s) of action for this compound may exist *in vivo*. On this note, anandamide affects multiple receptor systems in addition to the CB_1 receptor *in vitro*, including the capsaicin receptor (17) and gap junctions (18). Finally, a second endogenous lipid, 2-arachidonoyl glycerol, has been shown to bind and activate the CB_1

receptor (19, 20), indicating that natural ligands in addition to anandamide may exist for the CB_1 receptor.

The weak cannabinoid properties displayed by anandamide *in vivo* have been speculated to result from its rapid catabolism (1, 2, 14). Indeed, the half-life of anandamide *in vivo* appears to be on the order of minutes (21), severely hindering efforts to characterize the pharmacological and physiological function of this endogenous brain substance. Although several proteins and enzymes have been suggested to participate in the catabolism of anandamide (22–24), the roles that these proteins play in regulating anandamide levels and activity *in vivo* remain unknown. One candidate enzyme responsible for regulating anandamide function is fatty acid amide hydrolase (FAAH), a membrane-associated serine hydrolase enriched in brain and liver (22, 25–27). FAAH hydrolyzes anandamide and several other bioactive fatty acid amides *in vitro* (22, 28–31), including *N*-palmitoyl ethanolamine (32), a postulated endogenous ligand for CB-like receptors, and the sleep-inducing lipid oleamide (33). Here, we have tested the role that FAAH plays in controlling fatty acid amide levels and activity *in vivo* by generating and characterizing mice that possess a targeted disruption of the FAAH gene.

Materials and Methods

Generation of $FAAH^{-/-}$ Mice. The FAAH gene was isolated from a 129SvJ genomic library, and a 2.5-kb region encompassing the first exon was mapped and sequenced. A PGK-Neo cassette (consisting of a phosphoglycerate kinase promoter driving the neomycin phosphotransferase gene) was inserted between *Eco*RI and *Eco*RV sites located 2.3 kb apart, replacing the first FAAH exon (encoding amino acids 1–65) and ≈2 kb of upstream sequence. Homologous recombinant 129SvJ embryonic stem cell clones were identified by Southern analysis, and two such clones were used to generate chimeric mice on a C57BL/6 background. Chimeras from both clones gave germline transmission of the mutated gene. All mice used in this study were second or third generation offspring from intercrosses of 129SvJ-C57BL/6 $FAAH^{+/-}$ mice. Offspring from both clones were tested and provided indistinguishable results.
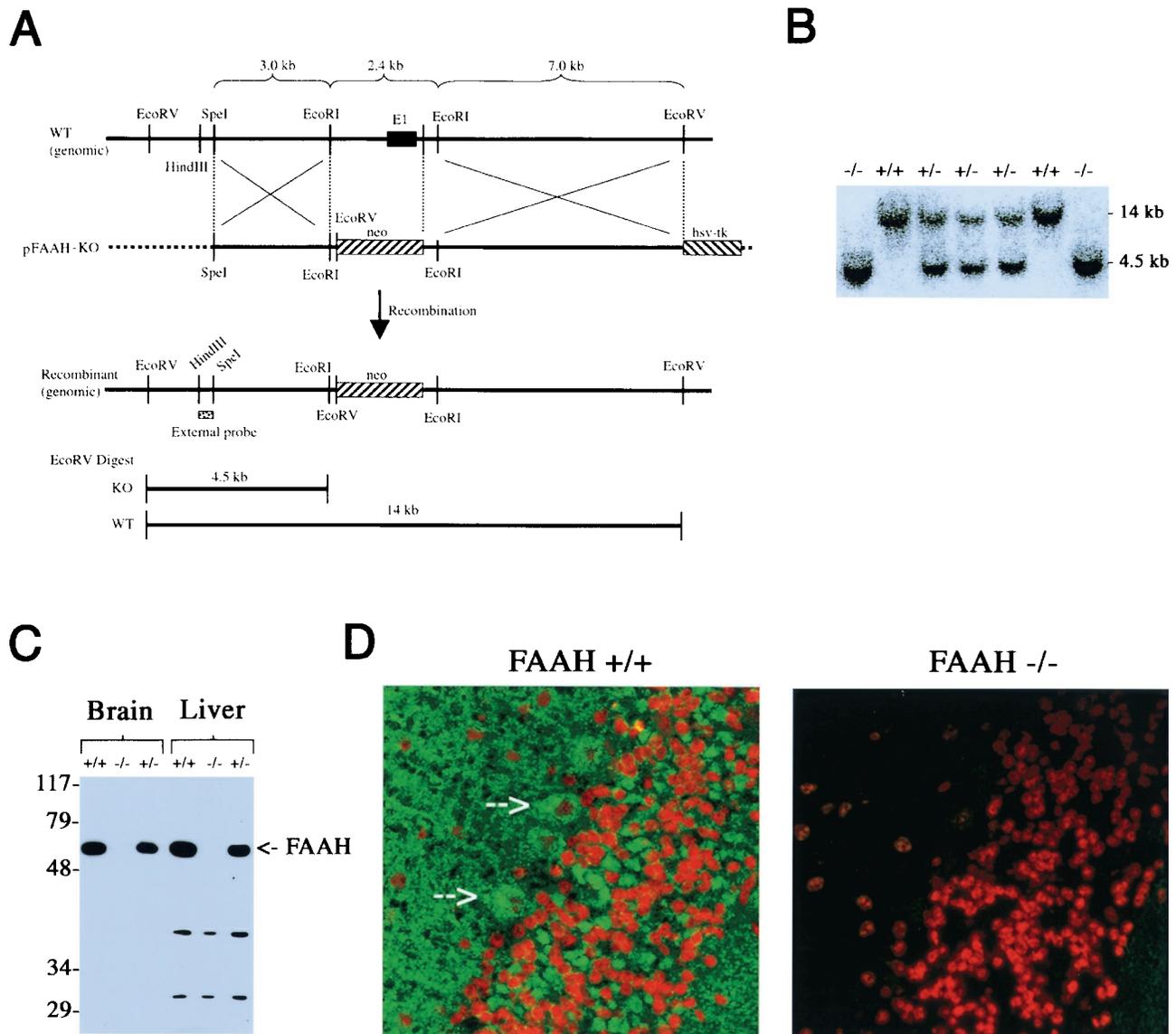
Biochemical and Cell Biological Studies. FAAH activity assays for oleamide and anandamide were measured by following the conversion of ^{14}C-labeled substrates using a TLC assay as described (27), with the exception that enzyme assays were

NEUROBIOLOGY

Fig. 1. Generation and biochemical characterization of FAAH$^{-/-}$ mice. (*A*) The genomic structure surrounding the deleted FAAH exon 1 (E1). Only relevant restriction sites are designated. The deleted E1 exon encodes amino acids 1–65 of the FAAH protein. (*B*) Southern blot analysis of *Eco*RV-digested genomic DNA by using the indicated probe (External probe in *A*), where 4.5- and 14-kb bands correspond to FAAH$^{-/-}$ and FAAH$^{+/+}$ genotypes, respectively. (*C*) Western blot analysis of tissues from FAAH$^{+/+}$, FAAH$^{+/-}$, and FAAH$^{-/-}$ mice demonstrating the selective absence of FAAH protein in FAAH$^{-/-}$ animals. (*D*) Confocal microscopy immunofluorescence images of cerebellar sections of FAAH$^{+/+}$ (*Left*) and FAAH$^{-/-}$ (*Right*) mice. Green signal, anti-FAAH; red signal, propidium iodide (stains nuclei). Arrowheads highlight intense FAAH immunoreactivity in the cell bodies of Purkinje neurons (*Left*).

conducted at pH 7.2. FAAH Western blots were conducted by using polyclonal anti-FAAH antibodies as described (26). For immunofluorescence images, mice were killed under deep anesthesia and brain samples were harvested for cryopreservation. The tissue was embedded in O.C.T. compound (Sakura/ TissueTek, Torrance, CA) and frozen on dry ice. Cryosections were cut in 5-μm steps, mounted on glass slides, and stored at $-80°C$ until needed. Slides were fixed at 37°C in 4% paraformaldehyde, hydrated in PBS, and blocked with 1% BSA in PBS. Blocked slides were washed with PBS and then incubated with anti-FAAH polyclonal antibodies (26, 34). Stained slides were then washed in PBS and incubated with secondary antibody directed against rabbit IgG and conjugated to Alexa 488 (Molecular Probes). Specimens were washed once more in PBS, counterstained with propidium iodide, and mounted in SloFade preservative (Molecular Probes). Stained slides were then ob-

served on a Zeiss Axiovert STV100 microscope with the Bio-Rad MRC100 confocal system. Imaging of both FAAH$^{+/+}$ and FAAH$^{-/-}$ specimens was performed with identical laser power and signal amplification settings.

Behavioral Studies. Locomotor activity was assessed by placing each mouse in a clear Plexiglas cage [18 × 10 × 8.5 inches (l × w × h)] that was marked in 7-cm-square grids on the floor of the cage. The number of grids that were traversed by the hind paws was counted from 15–20 min postinjection. Nociception was then assessed in the tail immersion assay, where each mouse was hand-held with ≈1 cm of the tip of the tail immersed into a water bath maintained at 56.0°C and the latency for the animal to withdraw its tail was scored. The cutoff was 15 s and the data are expressed as the percent maximum possible effect (%MPE), where %MPE $= 100 \cdot$ (postinjection latency $-$ preinjection

latency)/(15 − preinjection latency). Baseline thermal nociception was also analyzed, using the hot plate test, where the latency to jump or lick/shake a hind paw was scored. In the formalin assay, 20 μl of a 2.5% formalin solution were injected s.c. under the dorsal surface of the right hindpaw. The total licking time was recorded from 0–40 min after injection. The early phase of pain responses lasted from 0–5 min and the late phase lasted from 20–40 min. Catalepsy was evaluated by using the bar test, in which the front paws of each subject were placed on a rod (0.75 cm diameter) that was elevated 4.5 cm above the surface. Mice that remained motionless with their paws on the bar for 10 s (with the exception of respiratory movements) were scored as cataleptic. Rectal temperature was determined by inserting a thermocouple probe 1.2 cm into the rectum and temperature was obtained from a telethermometer. The preinjection rectal temperatures for FAAH$^{+/+}$ (35.6 $\pm$ 0.2°C, $n = 28$) and FAAH$^{-/-}$ (35.5 $\pm$ 0.1°C, $n = 30$) mice were equivalent. Catalepsy and rectal temperature were assessed at 60 min postinjection unless otherwise stated. The data reported are from a combination of male and female mice (no significant sex differences were observed for either genotype). All drugs were administered i.p. in a mixture of 1:1:18 ethanol:Emulphor:saline (10 μl/g body weight), except naloxone, which was administered i.p. in saline (SR141716A and THC kindly provided by the National Institute on Drug Abuse).

Measurement of Brain Levels of *N*-Acyl Ethanolamines (NAEs). NAE levels in the brains of FAAH$^{+/+}$ and FAAH$^{-/-}$ mice were quantified by isotope dilution liquid chromatography mass spectrometry (LC-MS) (16). Briefly, mice were anesthetized by using CO_2/O_2 and killed by decapitation. Brains were removed and immediately homogenized in a 2:1:1 mixture of chloroform:methanol:50 mM Tris, pH 8.0 containing *N*-oleoyl-d$_4$-ethanolamine and d$_4$-anandamide standards (0.5 nmol each per brain). The organic layer was removed, dried under N$_2$ gas, washed with ethyl acetate, and the washes transferred to a fresh glass vial and dried. The remaining residue was solubilized in methanol and injected onto an Agilent 1100 series LC-MS. Levels of endogenous NAEs were quantified by comparing their mass ion peak heights to those of the corresponding isotopically labeled standards. Standard curves were generated to confirm a linear relationship between peak height and NAE concentration. The anandamide data are shown in Fig. 6*A*. Endogenous brain levels of *N*-oleoyl ethanolamine were found to be 710 $\pm$ 90 and 18 $\pm$ 12 pmol/g tissue for FAAH$^{-/-}$ and FAAH$^{+/+}$ mice, respectively. Although a standard for *N*-palmitoyl ethanolamine was not included in the assay, a peak corresponding to the molecular mass of this lipid ($m/z = 300.3$) was greatly increased in FAAH$^{-/-}$ samples (relative to the included NAE standards), indicating that brain levels of this NAE were also up-regulated in these animals.

Results

Targeted Disruption of the FAAH Gene. To generate mice lacking FAAH, the first exon of the FAAH gene was removed by homologous recombination (Fig. 1 *A* and *B*). Western blotting with anti-FAAH antibodies confirmed the absence of FAAH protein in the brain and liver of FAAH knockout (FAAH$^{-/-}$) mice (Fig. 1*C*). Immunofluorescence analysis of cerebellar sections from FAAH$^{+/+}$ mice revealed intense staining in the cell bodies of Purkinje and granule neurons, as well as in the molecular layer, which contains the extensive Purkinje dendritic arbor (Fig. 1*D Left*). In contrast, no FAAH immunoreactivity was detected in cerebellar sections from FAAH$^{-/-}$ mice (Fig. 1*D Right*). These data confirm that FAAH is predominantly localized to the somatodendritic compartment of neurons in the central nervous system (34, 35). Importantly, brain and liver tissues from FAAH$^{-/-}$ mice also exhibited greatly reduced

Table 1. Anandamide and oleamide hydrolytic activities in FAAH$^{+/+}$, FAAH$^{+/-}$, and FAAH$^{-/-}$ mice (nmol/min/mg)

|		Anandamide hydrolysis	Oleamide hydrolysis
Brain	+/+	0.33 $\pm$ 0.04	0.24 $\pm$ 0.03
	+/−	0.20 $\pm$ 0.03	0.15 $\pm$ 0.01
	−/−	0.003 $\pm$ 0.002	0.004 $\pm$ 0.002
Liver	+/+	0.53 $\pm$ 0.06	0.54 $\pm$ 0.01
	+/−	0.29 $\pm$ 0.03	0.29 $\pm$ 0.07
	−/−	0.01 $\pm$ 0.01	0.03 $\pm$ 0.01

Fatty acid amide hydrolytic activities were measured as described in *Materials and Methods.*

FAAH catalytic activity (Table 1). For example, brain extracts from FAAH$^{-/-}$ mice hydrolyzed anandamide and oleamide 50–100-fold more slowly than brain extracts from FAAH$^{+/+}$ mice.

**Characterization of the Behavioral Responses Elicited by Anandamide in FAAH$^{+/+}$ and FAAH$^{-/-}$ Mice.** FAAH$^{-/-}$ mice were born at the expected Mendelian frequency and were viable, fertile, and largely indistinguishable from wild-type littermates. No differences were observed in general appearance, body weight, locomotion, or overt behavior. The role of FAAH in regulating anandamide activity *in vivo* was investigated by comparing responses of FAAH$^{+/+}$ and FAAH$^{-/-}$ mice to anandamide in neurobehavioral assays that measured spontaneous activity, thermal pain sensation, catalepsy, and rectal temperature. Over the dose range tested (6.25–50 mg/kg, i.p. administration), anandamide failed to produce any significant effects in FAAH$^{+/+}$ mice (Fig. 2 *A–D*). Considering that anandamide has been previously found to induce modest, but significant cannabinoid pharmacology in some strains of mice (10, 11), the absence of any activity for anandamide in the FAAH$^{+/+}$ mice studied here may be due to strain differences. In contrast to wild-type mice, FAAH$^{-/-}$ mice exhibited robust, dose-dependent behavioral responses to anandamide, displaying hypomotility (Fig. 2*A*), analgesia (*B*), catalepsy (*C*), and hypothermia (*D*). At the highest dose tested (50 mg/kg), anandamide induced in FAAH$^{-/-}$ mice an 84 $\pm$ 8% reduction in spontaneous activity, profound analgesia in the tail immersion test (89 $\pm$ 11% maximum possible effect), strong cataleptic behavior in the bar test (88% of the test group), and a 7.9 $\pm$ 0.3°C reduction in rectal temperature.

The striking impact of anandamide (12.5–50 mg/kg, i.p.) on the behavior of FAAH$^{-/-}$ mice was readily detected within 5 min of treatment, at which time the animals adopted a flattened, rigid posture and remained completely motionless with their eyes open. If startled by sound or touch, these mice would react with brief fits of spastic movement before quickly reentering a flattened, immobile state. Anandamide-treated FAAH$^{-/-}$ mice remained immobile for 2–4 hours (depending on dose), after which they gradually reinitiated normal cage activities (e.g., movement, rearing, grooming). The duration of anandamide's behavioral effects in FAAH$^{-/-}$ mice was further examined by measuring rectal temperature and catalepsy at various times posttreatment. Coinciding closely with their overt cage behavior, anandamide-treated FAAH$^{-/-}$ mice (50 mg/kg, i.p.) showed a robust drop in rectal temperature that peaked between 1 and 2 h posttreatment and began to return to wild-type values by 4 h (Fig. 3*A*). Likewise, catalepsy was most extreme at 1 h posttreatment and gradually dissipated by 4 h (Fig. 3*B*). FAAH$^{-/-}$ mice were indistinguishable from FAAH$^{+/+}$ mice when analyzed 24 h after treatment with anandamide.

NEUROBIOLOGY
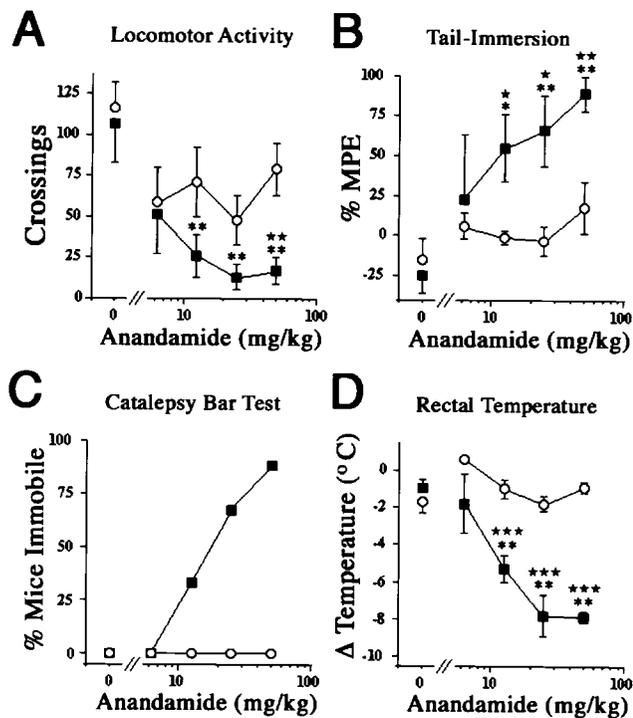
Fig. 2. Pharmacological activity of anandamide in FAAH$^{+/+}$ and FAAH$^{-/-}$ mice. Anandamide elicited dose-dependent pharmacological effects in FAAH$^{-/-}$ mice (■), but failed to produce any significant effects in FAAH$^{+/+}$ mice (○). (*A*) Hypomotility (locomotor activity), ED$_{50}$ < 6.25 mg/kg; (*B*) antinociception (tail-immersion), ED$_{50}$ [95% confidence limits (CL)] = 13 (5–30) mg/kg; (*C*) catalepsy, ED$_{50}$ (95% CL) = 20 (11–35) mg/kg; (*D*) hypothermia (rectal temperature), ED$_{50}$ (95% CL) = 11 (6–19) mg/kg. ⋆, P < 0.05; ⋆⋆, P < 0.01; and ⋆⋆⋆, P < 0.001, for FAAH$^{-/-}$ versus FAAH$^{+/+}$ mice receiving the same treatment (planned comparison). ∗, P < 0.05 and ∗∗, P < 0.01 for anandamide-treated versus vehicle-treated FAAH$^{-/-}$ mice (Dunnett's test). The results are presented as means ± SE. n = 6–8 mice per group.

The Behavioral Effects of Anandamide in FAAH$^{-/-}$ Mice Are CB$_1$-Dependent. The intense behavioral effects induced by anandamide in FAAH$^{-/-}$ mice were reminiscent of those traditionally observed in rodents treated with THC (11), suggesting that anandamide may indeed act as an endogenous CB$_1$ ligand. To determine the contribution of CB$_1$ receptor pathways to the behavioral pharmacology elicited by anandamide in FAAH$^{-/-}$
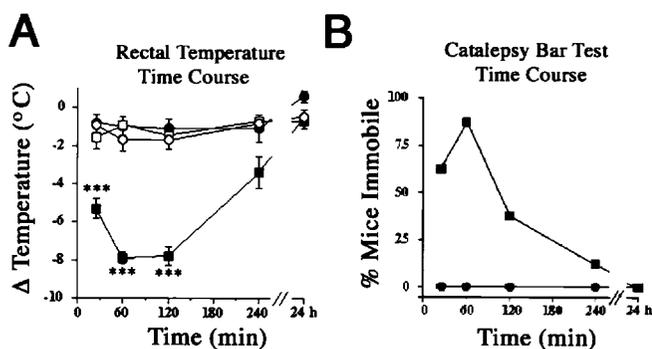
Fig. 3. Time course of the hypothermia (*A*) and catalepsy (*B*) in mice treated with either vehicle (FAAH$^{+/+}$, open circles; FAAH$^{-/-}$, filled circles) or 50 mg/kg anandamide (□, FAAH$^{+/+}$; ■ FAAH$^{-/-}$). ∗∗∗, P < 0.001 for anandamide-treated FAAH$^{-/-}$ mice versus the other three test groups (Scheffé test). The results are presented as means ± SE. n = 6–8 mice per group.
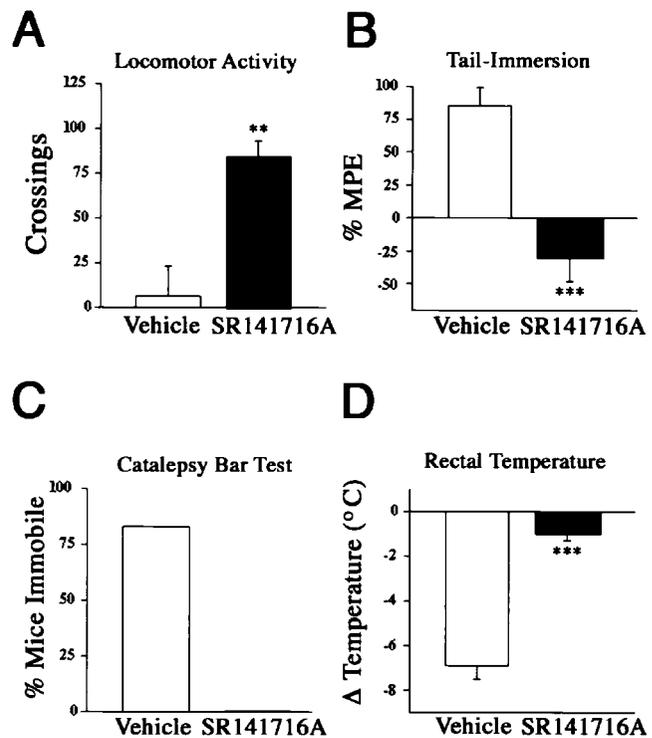
Fig. 4. The behavioral effects of anandamide in FAAH$^{-/-}$ mice are mediated by the CB$_1$ cannabinoid receptor. The effect of vehicle (open bars) or SR141716A (filled bars) administered 10 min before treatment with anandamide in FAAH$^{-/-}$ mice. SR141716A (10 mg/kg) completely blocked the hypomotility (*A*), antinociception (*B*), catalepsy (*C*), and hypothermia (*D*) induced by anandamide (50 mg/kg), as SR141716A-pretreated, anandamide-treated FAAH$^{-/-}$ mice were indistinguishable in all behavioral assays from FAAH$^{-/-}$ mice treated with vehicle alone (0 mg/kg anandamide data in Fig. 2 *A–D*). ∗∗, P < 0.01 and ∗∗∗, P < 0.001 for SR141716A-treated versus vehicle-treated FAAH$^{-/-}$ mice (planned comparison). The results are presented as means ± SE. n = 6–8 mice per group.

mice, these animals were administered the CB$_1$ antagonist SR141716A (10 mg/kg, i.p.) 10 min before treatment with anandamide (50 mg/kg, i.p.). Remarkably, all of anandamide's behavioral effects in FAAH$^{-/-}$ mice were completely blocked by pretreatment with SR141716A (Fig. 4 *A–D*). In contrast, pretreatment with the opioid receptor antagonist naloxone (2 mg/kg, i.p.) failed to reduce any of anandamide's activities in FAAH$^{-/-}$ mice (data not shown). The ED$_{50}$ values (mg/kg) for SR141716A-based antagonism of the behavioral effects of anandamide in FAAH$^{-/-}$ mice were: for hypomotility, 1.2 [0.3–4.9 (95% confidence limits)]; for thermal analgesia, 1.2 (0.8–2.0); for catalepsy, 0.8 (0.5–1.5); and for hypothermia, 1.3 (0.6–3.0). These values are nearly identical to those reported previously for the antagonism of the behavioral effects of exogenous cannabinoid ligands by SR141716A (36), strongly supporting the notion that the observed behavioral effects of anandamide in FAAH$^{-/-}$ mice occur predominantly, if not exclusively through the CB$_1$ receptor. The profound CB$_1$-dependent pharmacological effects induced by anandamide in FAAH$^{-/-}$ mice initially suggested that a sensitized or up-regulated CB$_1$ receptor system might exist in these animals. However, FAAH$^{-/-}$ and FAAH$^{+/+}$ mice exhibited similar THC dose-response profiles for all of the behavioral assays tested (Table 2), indicating that their CB$_1$ receptors were functionally equivalent. Collectively, these data indicate that in the absence of FAAH, anandamide acts as potent and selective CB$_1$ agonist *in vivo*.

Table 2. ED₅₀ values for the behavioral effects of THC in FAAH⁺/⁺ and FAAH⁻/⁻ mice [mg/kg (95% confidence limits)]

|	Hypomotility	Antinociception	Hypothermia
FAAH⁺/⁺	13 (10–17)	13 (7–26)	12 (9–17)
FAAH⁻/⁻	13 (9–18)	12 (7–20)	15 (10–24)

FAAH⁺/⁺ and FAAH⁻/⁻ mice were injected with 5, 10, 20, or 40 mg/kg THC (i.p.) and tested as described in *Materials and Methods*. The highest dose of THC failed to elicit more than 50% catalepsy in either genotype. $n = 6-8$ mice per group.

FAAH⁻/⁻ Mice Exhibit Reduced Pain Sensitivity. During the course of characterizing the pharmacological effects of anandamide in FAAH⁺/⁺ and FAAH⁻/⁻ mice, baseline measures of spontaneous activity, rectal temperature, and pain sensitivity were recorded. FAAH⁻/⁻ mice did not differ from FAAH⁺/⁺ mice in terms of their respective locomotor activities or rectal temperatures (Fig. 2 *A* and *D*). However, FAAH⁻/⁻ mice were found to display altered thermal pain sensation, exhibiting prolonged response latencies in both the tail immersion and hot plate tests when compared with both FAAH⁺/⁺ and FAAH⁺/⁻ mice (Fig. 5*A Left* and Fig. 6*B*). In the hot plate test, FAAH⁻/⁻ mice differed significantly from FAAH⁺/⁺ mice over a restricted temperature range (Fig. 5*A Right*). Interestingly, a similar phenotype was observed in the substance P/neurokinin A knockout mouse and interpreted to implicate these peptides in neural pathways that communicate moderate to intense pain stimuli (37). To examine whether other forms of pain sensation were also altered in FAAH⁻/⁻ mice, these animals were compared with FAAH⁺/⁺ and FAAH⁺/⁻ mice in the formalin test for chemical pain sensation. FAAH⁻/⁻ mice exhibited a significant reduction in pain behavior during the first phase of the formalin test relative to both FAAH⁺/⁺ and FAAH⁺/⁻ mice (Fig. 5*B*). A similar trend of reduced pain responses in FAAH⁻/⁻ mice was also observed in the second phase of the formalin test, but these data just failed to reach significance ($P = 0.055$ for FAAH⁻/⁻ versus FAAH⁺/⁺ mice, planned comparison). Collectively, these results implicate FAAH in the regulation of mammalian behavioral responses to multiple forms of pain stimuli.

FAAH⁻/⁻ Mice Possess Enhanced Endogenous Cannabinoid Levels and Activity. The reduced pain perception exhibited by FAAH⁻/⁻ mice suggested that these animals might possess enhanced endogenous cannabinoid activity. To explore this notion further,
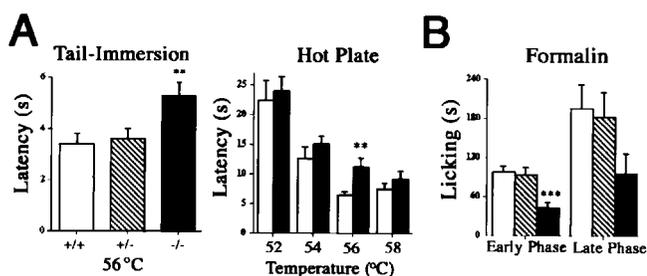
Fig. 5. Altered pain responses in FAAH⁻/⁻ mice. (*A*) FAAH⁻/⁻ mice (filled columns) exhibited prolonged response latencies in both the tail-immersion ($n = 48$, 50, and 62 for FAAH⁺/⁺, FAAH⁺/⁻, and FAAH⁻/⁻ genotypes, respectively) and hot plate ($n = 12-15$ mice per group) tests for thermal pain sensation relative to FAAH⁺/⁺ (open columns) and FAAH⁺/⁻ mice (hatched bars; for hot plate data with FAAH⁺/⁻ mice, see Fig. 6*B Left*). (*B*) Duration of licking during the early phase of the formalin test was reduced in FAAH⁻/⁻ mice (filled columns) relative to FAAH⁺/⁻ (hatched columns) and FAAH⁺/⁺ (open columns) mice; $n = 8-10$ mice per group. **, $P < 0.01$ and ***, $P < 0.001$ for FAAH⁻/⁻ versus FAAH⁺/⁻ or FAAH⁺/⁺ mice (planned comparisons). The results are presented as means ± SE.
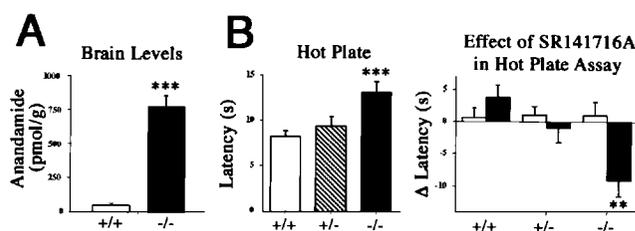
Fig. 6. Enhanced endogenous cannabinoid levels and activity in FAAH⁻/⁻ mice. (*A*) FAAH⁻/⁻ mice (filled column) possessed greatly increased endogenous brain levels of anandamide relative to FAAH⁺/⁺ mice (open bar); FAAH⁺/⁺, 50 ± 10 pmol/g of tissue; FAAH⁻/⁻, 775 ± 113 pmol/g of tissue; ***, $P < 0.001$ for FAAH⁻/⁻ versus FAAH⁺/⁺ mice (planned comparison); $n = 7-8$ mice per group. (*B*) The prolonged response latency of FAAH⁻/⁻ mice in the hot plate assay (*Left*, filled bar) was reversed by treatment with SR141716A (*Right*, filled bar). Vehicle administration failed to significantly affect the response latencies of FAAH⁻/⁻, FAAH⁺/⁻, and FAAH⁺/⁺ mice (*Right*, open bars), and SR141716A failed to significantly affect the response latencies of FAAH⁺/⁻ and FAAH⁺/⁺ mice (*Right*, filled bars). $n = 8-11$ mice per group, assayed 30 min posttreatment. **, $P \leq 0.01$ for SR141716A-treated FAAH⁻/⁻ mice versus either vehicle-treated FAAH⁻/⁻ mice or baseline latencies (planned comparison); ***, $P < 0.005$, for FAAH⁻/⁻ versus FAAH⁺/⁻ or FAAH⁺/⁺ mice (planned comparison). The results are presented as means ± SE.

brain levels of anandamide and related NAEs were measured by isotope dilution liquid chromatography mass spectrometry (LC-MS). Strikingly, brains from FAAH⁻/⁻ mice possessed 15-fold higher levels of anandamide than brains from FAAH⁺/⁺ mice (Fig. 6*A*). Other NAEs, including *N*-oleoyl and *N*-palmitoyl ethanolamine, were similarly up-regulated (see *Materials and Methods*), consistent with shared biosynthetic and degradative pathways for these lipids (38). To test whether enhanced levels of endogenous anandamide might be responsible for the analgesia observed in FAAH⁻/⁻ mice, the pain responses of these animals, FAAH⁺/⁺, and FAAH⁺/⁻ mice were tested in the hot plate test both before and after treatment with either vehicle or SR141716A (Fig. 6*B*). No significant changes from baseline were observed for the hot plate response latencies of vehicle-treated FAAH⁺/⁺, FAAH⁺/⁻, and FAAH⁻/⁻ mice, or in SR141617A-treated FAAH⁺/⁺ and FAAH⁺/⁻ mice (Fig. 6*B Right*). In sharp contrast to all of these test groups, FAAH⁻/⁻ mice treated with SR141716A showed a dramatic reduction in their pain response latencies (Fig. 6*B Right*), indicating that a substantial fraction of their altered pain sensation was mediated by CB₁ receptor pathways.

Discussion

Efforts to date to determine the endogenous functions of anandamide have been thwarted by its short half-life *in vivo* ($t_{1/2} < 5$ min) (21). Although several proteins have been suggested to participate in the rapid catabolism of anandamide (22–24), our results show that anandamide signaling *in vivo* is primarily regulated by a single degradative enzyme, FAAH. In FAAH⁻/⁻ mice, anandamide generated robust CB₁ receptor-dependent behavioral effects that rivaled those of THC in terms of efficacy and duration. Additionally, FAAH⁻/⁻ mice possessed dramatically elevated endogenous brain levels of anandamide and exhibited reduced pain behavior that was reversed by the CB₁ antagonist SR141716A. Collectively, these data indicate that anandamide is a potent and selective CB₁ ligand *in vivo*, participating in a FAAH-regulated endogenous cannabinoid tone that modulates mammalian pain responses.

It is intriguing that anandamide appears to have acted as such a selective CB₁ agonist in FAAH⁻/⁻ mice, especially considering that this compound was recently reported to produce significant behavioral effects in CB₁⁻/⁻ mice (16). The lack of any observed SR141716A-insensitive activity for anandamide in FAAH⁻/⁻

mice might suggest that its other potential sites of action have been down-regulated in the absence of FAAH. However, additional interpretations of this finding are possible. For example, anandamide has recently been shown to induce SR141716A-sensitive vasodilation in $CB_1^{-/-}/CB_2^{-/-}$ mice (39), indicating that other, as yet unidentified CB-like receptors may exist for anandamide *in vivo*. Alternatively, much of the apparent CB_1-independent pharmacology exhibited by anandamide in wild-type animals could be mediated by arachidonic acid-based metabolites that accumulate as a result of the rapid, FAAH-catalyzed hydrolysis of anandamide *in vivo*. The generation and characterization of $FAAH^{-/-}/CB_1^{-/-}$ mice may help to clarify these issues.

Finally, when one considers the vast number of proteases, amidases, and lipases that exist in mammalian organisms (over 300 such enzymes are encoded by the human genome; refs. 40 and 41), it is remarkable that the catabolism of fatty acid amides is so tightly controlled by a single enzyme. Considering that FAAH regulates both the amplitude and duration of anandamide's biological activity, inhibitors of this enzyme (42) may serve as valuable pharmaceutical agents for the treatment of pain and neuropsychiatric disorders.

1. Pop, E. (1999) *Curr. Opin. Chem. Biol.* **3,** 418–425.
2. Piomelli, D., Giuffrida, A., Calignano, A. & Rodriguez de Fonseca, F. (2000) *Trends Pharmacol. Sci.* **21,** 218–224.
3. Martin, B. R., Mechoulam, R. & Razdan, R. K. (1999) *Life Sci.* **65,** 573–595.
4. Mechoulam, R. (1986) *Cannabinoids as Therapeutic Agents* (CRC, Boca Raton, FL), pp. 1–19.
5. Pertwee, R. G. (1997) *Pharmacol. Ther.* **74,** 129–180.
6. Devane, W. A., Hanus, L., Breuer, A., Pertwee, R. G., Stevenson, L. A., Griffin, G., Gibson, D., Mandelbaum, A., Etinger, A. & Mechoulam, R. (1992) *Science* **258,** 1946–1949.
7. Felder, C. C., Briley, E. M., Axelrod, J., Simpson, J. T., Mackie, K. & Devane, W. A. (1993) *Proc. Natl. Acad. Sci. USA* **90,** 7656–7660.
8. Walker, J. M., Huang, S. M., Strangman, N. M., Tsou, K. & Sanudo-Pena, M. C. (1999) *Proc. Natl. Acad. Sci. USA* **96,** 12198–12203.
9. Crawley, J. N., Corwin, R. L., Robinson, J. K., Felder, C. C., Devane, W. A. & Axelrod, J. (1993) *Pharmacol. Biochem. Behav.* **46,** 967–972.
10. Fride, E. & Mechoulam, R. (1993) *Eur. J. Pharmacol.* **231,** 313–314.
11. Smith, P. B., Compton, D. R., Welch, S. P., Razdan, R. K., Mechoulam, R. & Martin, B. R. (1994) *J. Pharmacol. Exp. Ther.* **270,** 219–227.
12. Childer, S. R., Sexton, T. & Roy, M. B. (1994) *Biochem. Pharmacol.* **47,** 711–715.
13. Terranova, A. E., Michaud, C., Le Fur, G. & Soubrie, P. (1995) *Nauyn Schmiedeberg's Arch. Pharmacol.* **352,** 576–579.
14. Adams, I. B., Compton, D. R. & Martin, B. R. (1998) *J. Pharmacol. Exp. Ther.* **284,** 1209–1217.
15. Costa, B., Vailati, S. & Colleoni, M. (1999) *Behav. Pharmacol.* **10,** 327–331.
16. Di Marzo, V., Breivogel, C. S., Tao, Q., Bridgen, D. T., Razdan, R. K., Zimmer, A. M., Zimmer, A. & Martin, B. R. (2000) *J. Neurochem.* **75,** 2434–2444.
17. Zygmunt, P. M., Petersson, J., Andersson, D. A., Chuang, H., Sorgard, M., Di Marzo, V., Julius, D. & Hogestatt, E. D. (1999) *Nature (London)* **400,** 452–457.
18. Venance, L., Piomelli, D., Glowinski, J. & Glaume, C. (1995) *Nature (London)* **376,** 590–592.
19. Mechoulam, R., Ben-Shabat, S., Hanus, L., Ligumsky, M., Kaminski, N. E., Schatz, A. R., Gopher, A., Almog, S., Martin, B. R., Compton, D. R., *et al.* (1995) *Biochem. Pharmacol.* **50,** 83–90.
20. Sugiura, T., Kondo, S., Sukagawa, A., Nakane, S., Shinoda, A., Itoh, K., Yamashita, A. & Waku, K. (1995) *Biochem. Biophys. Res. Commun.* **215,** 89–97.
21. Willoughby, K. A., Moore, S. F., Martin, B. R. & Ellis, E. F. (1997) *J. Pharmacol. Exp. Ther.* **282,** 243–247.
22. Cravatt, B. F., Giang, D. K., Mayfield, S. P., Boger, D. L., Lerner, R. A. & Gilula, N. B. (1996) *Nature (London)* **384,** 83–87.
23. Beltramo, M., Stella, N., Calignano, A., Lin, S. Y., Makriyannis, A. & Piomelli, D. (1997) *Science* **277,** 1094–1097.
24. Ueda, N., Yamanaka, K., Terasawa, Y. & Yamamoto, S. (1999) *FEBS Lett.* **454,** 267–270.
25. Giang, D. K. & Cravatt, B. F. (1997) *Proc. Natl. Acad. Sci. USA* **94,** 2238–2242.
26. Patricelli, M. P., Lashuel, H. A., Giang, D. K., Kelly, J. W. & Cravatt, B. F. (1998) *Biochemistry* **37,** 15177–15187.
27. Patricelli, M. P., Lovato, M. A. & Cravatt, B. F. (1999) *Biochemistry* **38,** 9804–9812.
28. Deutsch, D. G. & Chin, S. A. (1993) *Biochem. Pharmacol.* **46,** 791–796.
29. Maurelli, S., Bisogno, T., De Petrocellis, L., Di Luccia, A., Marino, G. & Di Marzo, V. (1995) *FEBS Lett.* **377,** 82–86.
30. Ueda, N., Kurahashi, Y., Yamamoto, S. & Tokunaga, T. (1995) *J. Biol. Chem.* **270,** 23823–23827.
31. Desarnaud, F., Cadas, H. & Piomelli, D. (1995) *J. Biol. Chem.* **270,** 6030–6035.
32. Calignano, A., La Rana, G., Giuffrida, A. & Piomelli, D. (1998) *Nature (London)* **394,** 277–281.
33. Cravatt, B. F., Prospero-Garcia, O., Siuzdak, G., Gilula, N. B., Henriksen, S. J., Boger, D. L. & Lerner, R. A. (1995) *Science* **268,** 1506–1509.
34. Egertova, M., Giang, D. K., Cravatt, B. F. & Elphick, M. R. (1998) *Proc. R. Soc. London Ser. B* **265,** 2081–2085.
35. Tsou, K., Nogueron, M. I., Muthian, S., Sanudo-Pena, M. C., Hillard, C. J., Deutsch, D. G. & Walker, J. M. (1998) *Neurosci. Lett.* **254,** 137–140.
36. Rinaldi-Carmona, M., Barth, F., Heaulme, M., Shire, D., Calandra, B., Congy, C., Martinez, S., Maruani, J., Neliat, G., Caput, D., *et al.* (1994) *FEBS Lett.* **350,** 240–244.
37. Cao, Y. Q., Mantyh, P. W., Carlson, E. J., Gillespie, A.-M., Epstein, C. J. & Basbaum, A. I. (1996) *Nature (London)* **392,** 390–394.
38. Di Marzo, V., Fontana, A., Cadas, H., Schinelli, S., Cimino, G., Schwartz, J.-C. & Piomelli, D. (1994) *Nature (London)* **372,** 686–691.
39. Jarai, Z., Wagner, J. A., Varga, K., Lake, K. D., Compton, D. R., Martin, B. R., Zimmer, A. M., Bonner, T. I., Buckley, N. E., Mezey, E., *et al.* (1999) *Proc. Natl. Acad. Sci. USA* **96,** 14136–14141.
40. Lander, E. S., Linton, L. M., Birren, B., Nusbaum, C., Zody, M. C., Baldwin, J., Devon, K., Dewar, K., Doyle, M., FitzHugh, W., *et al.* (2001) *Nature (London)* **409,** 860–921.
41. Venter, J. C., Adams, M. D., Myers, E. W., Li, P. W., Mural, R. J., Sutton, G. G., Smith, H. O., Yandell, M., Evans, C. A., Holt, R. A., *et al.* (2001) *Science* **291,** 1304–1351.
42. Boger, D. L., Sato, H., Lerner, A. E., Hedrick, M. P., Fecik, R. A., Miyauchi, H., Wilkie, G. D., Austin, B. J., Patricelli, M. P. & Cravatt, B. F. (2000) *Proc. Natl. Acad. Sci. USA* **97,** 5044–5049.